AEM Accepted Manuscript Posted Online 21 August 2015 Appl. Environ. Microbiol. doi:10.1128/AEM.02280-15 Copyright © 2015, American Society for Microbiology. All Rights Reserved.

1	Quantitative Microbial Ecology Through Stable Isotope Probing			
2				
3	Bruce A. Hungate ^{a,b,#} , Rebecca L. Mau ^a , Egbert Schwartz ^{a,b} , J. Gregory Caporaso ^{a,b}			
4	Paul Dijkstra ^{a,b} , Natasja van Gestel ^a , Benjamin J. Koch ^a , Cindy M. Liu ^{d,e} , Theresa A			
5	McHugh ^{a*} , Jane C. Marks ^{a,b} , Ember Morrissey ^{a,b} , Lance B. Price ^{d,f}			
6				
7				
8	^a Center for Ecosystem Science and Society, Northern Arizona University, Flagstaff,			
9	Arizona, USA; ^b Department of Biological Sciences, Northern Arizona University,			
10	Flagstaff, Arizona, USA; ^c Center for Microbial Genetics and Genomics, Northern			
11	Arizona University, Flagstaff, Arizona, USA; ^d Translational Genomics Research Center			
12	Flagstaff Arizona, USA; eDepartment of Pathology, Johns Hopkins School of Medicine			
13	Baltimore, Maryland, USA; ^f Department of Environmental and Occupational Health,			
14	Milken Institute School of Public Health, George Washington University, Washington,			
15	District of Columbia, USA			
16				
17	#Address correspondence to Bruce Hungate, Bruce.Hungate@nau.edu			
18				
19	*Present address: U.S. Geological Survey, Southwest Biological Science Center, Moab,			
20	Utah, USA			
21				
22	Running head: Quantitative Stable Isotope Probing			
23				

24 **Abstract**

25

26

27

28

29

30

31

32

33

34

35

36

37

38

39

40

41

42

43

44

45

Bacteria grow and transform elements at different rates, yet quantifying this variation in the environment is difficult. Determining isotope enrichment with fine taxonomic resolution after exposure to isotope tracers could help, but there are few suitable techniques. We propose a modification to Stable Isotope Probing (SIP) that enables determining the isotopic composition of DNA from individual bacterial taxa after exposure to isotope tracers. In our modification, after isopycnic centrifugation, DNA is collected in multiple density fractions, and each fraction is sequenced separately. Taxon specific density curves are produced for labeled and non-labeled treatments, from which the shift in density for each individual taxon in response to isotope labeling is calculated. Expressing each taxon's density shift relative to that taxon's density measured without isotope enrichment accounts for the influence of nucleic acid composition on density and isolates the influence of isotope tracer assimilation. The shift in density translates quantitatively to isotopic enrichment. Because this revision to SIP allows quantitative measurements of isotope enrichment, we propose to call it quantitative Stable Isotope Probing (qSIP). We demonstrate qSIP using soil incubations, in which soil bacteria exhibited strong taxonomic variation in ¹⁸O and ¹³C composition after exposure to ¹⁸O-H₂O or ¹³C-glucose. Addition of glucose increased assimilation of ¹⁸O into DNA from ¹⁸O-H₂O. However, the increase in ¹⁸O assimilation was greater than expected based on utilization of glucose-derived carbon alone, because glucose addition indirectly stimulated bacteria to utilize other substrates for growth. This example illustrates the benefit of a quantitative approach to stable isotope probing.

- Keywords: stable isotope probing, oxygen-18, ¹⁸O-H₂O, biodiversity, ecosystem 46
- functioning, soil carbon cycle 47

Introduction

48

49

50

51

52

53

54

55

56

57

58

59

60

61

62

63

64

65

66

The types of organisms present in an ecosystem profoundly influence its functioning, an idea well established for plants and animals, formalized in the state factor theory of ecosystem science (1), and illustrated through the impacts of plant and animal invasions on ecosystem processes (2). The physiological and taxonomic diversity of microorganisms far exceeds that of plants and animals combined (3). Yet, despite progress applying molecular tools to analyze microbial diversity of intact assemblages (4-6), our understanding of how individual microbial taxa affect ecosystem processes like element cycling remains weak. When applied to intact microbial assemblages, stable isotope probing (SIP) partly addresses this challenge, in that it links physically the fluxes of elements to an organism's genome. In conventional SIP, organisms that utilize isotopically labeled substrates incorporate the heavy isotope into their nucleic acids, increasing the density of those nucleic acids which then migrate further along a cesium chloride density gradient formed during isopycnic centrifugation. This enables identifying organisms that utilized the labeled compound for growth (7). Conventional SIP applications use a qualitative approach that identifies visually the separation caused by isotope incorporation (7). Nucleic acids in density regions defined as "heavy" or "light" are then sequenced. Organisms disproportionately represented in the "heavy" region are interpreted as having utilized the labeled substrate for growth (8-11).

67

68

69

70

SIP is a robust technique to identify microbial populations that assimilate a labeled substrate, but it does not provide quantitative measures of assimilation rates, for three reasons. First, the distinction between labeled and unlabeled organisms is binary, defined

72

73

74

75

76

77

78

79

80

81

82

83

84

85

86

87

88

89

90

91

92

93

by the density regions selected by the investigator, limiting the resolution of taxonspecific responses to labeled or unlabeled. Second, the distribution of DNA along the density gradient reflects the influences of both isotope incorporation and GC (guanine plus cytosine) content because the density of DNA increases with its GC content (12). Any comparison of density regions will reflect both influences, challenging inferences about quantitative isotope incorporation. Third, in conventional SIP there are no assurances that the identification of the labeled community is complete. Low GC content organisms that incorporated the isotope label may not have shifted sufficiently in density to be part of the "labeled" density fraction, and high GC content organisms that did not incorporate the label may be erroneously inferred to be part of the labeled community. This could result in incomplete coverage when discrete, non-contiguous, density intervals representing "heavy" and "light" fractions (13, 14) are selected for sequencing, omitting information about the microbial assemblage contained in the DNA at intermediate densities. In other cases, only the "heavy" fractions in both labeled and unlabeled treatments were sequenced and compared: any new organisms that appeared in the heavy fraction of the labeled treatment were inferred to have taken up enough of the isotope tracer to have shifted the density of their DNA (15). This approach could have excluded organisms that incorporated the isotope tracer, but did not shift sufficiently to be represented in the "heavy" fraction, because of their low GC content. In these ways, SIP as typically practiced is a qualitative technique capable of identifying some of the organisms that utilize a substrate, not a quantitative one capable of exploring the full range of variation in isotope incorporation among microbial taxa.

95

96

97

98

99

100

101

102

103

104

105

106

107

108

109

110

111

112

113

114

115

116

Here, we describe modifications to SIP that enable quantifying isotopic incorporation into the genomes of individual taxa. We developed an approach that quantifies the baseline density of the DNA of individual taxa without exposure to isotope tracers, and then quantifies the change in DNA density of each taxon caused by isotope incorporation. Using a model of isotope substitution in DNA, we convert the observed change in density to isotope composition. We show how qSIP applies in soil incubations using a specific carbon source (13C-glucose) and using a universal substrate for growing organisms (18O-H₂O). We also show how combining these tracers provides insight into the microbial ecology of a biogeochemical phenomenon widely observed in soil, the priming effect (16). The "priming effect" is the phenomenon where there occurs "extra decomposition of native soil organic matter in a soil receiving an organic amendment" (17), first documented over 80 years ago (18-20). The opposite can also be found, where substrate addition suppresses organic matter mineralization (21). Some hypotheses to explain priming invoke microbial biodiversity (22), yet those controls remain cryptic, in part because of the difficulty of identifying organisms that respond indirectly to substrate addition by increasing decomposition of native soil organic matter. Quantitative SIP has the potential to address these phenomena, by parsing out the contributions of specific microorganisms to decomposition of the added substrate, labeled with ¹³C, and to the decomposition of native soil organic matter, which an ¹⁸O-H₂O label can detect. Furthermore, the determination of taxon-specific isotope enrichment for each element in qSIP lays the foundation for ascribing rates of element fluxes to particular organisms, which could help explain C fluxes in priming, typically measured on a soil mass basis (e.g., µg C g soil⁻¹ d⁻¹). In this way, this example illustrates the potential of qSIP to

Applied and Environmental Microbiology

- advance microbial ecology as a quantitative field, relating microbial biodiversity to 117
- 118 element cycling at the ecosystem scale.
- 119

120 Methods

121

122

123

124

125

126

127

128

129

130

131

132

133

134

135

136

137

138

139

140

141

Soil incubations and DNA extractions

Our sample processing scheme, from soil collection, nucleic acid extraction, centrifugation, to data analysis, is summarized in Figure 1. Soil (0-15 cm) was collected in November 2012 from a ponderosa pine forest meadow, located on the C. Hart Merriam Elevation Gradient in Northern Arizona, **USA** (35.42N,-111.67W; http://nau.edu/ecoss/what-we-do/future-ecosystems/elevation-gradient-experiment/). Soil was sieved (2 mm mesh), left to air-dry for 96 hours, then stored at 4°C before the experiment started. One gram of soil was added to 15 mL Falcon tubes and adjusted to 60% water holding capacity, incubated for one week, and then allowed to air dry for 48 hours prior to isotope additions. Samples were incubated for 7 days. During the incubation, samples received 200 µL of water g⁻¹ soil or a glucose solution at a concentration of 500 μg C $g^{\text{-1}}$ soil in the following isotope and substrate treatments (each with n=3): 1) water at natural abundance δ^{18} O; 2) δ^{18} O-enriched water (atom fraction 97%); 3) glucose and water at natural abundance δ^{13} C and δ^{18} O; 4) 13 C-enriched glucose (atom fraction 99%) and water at natural abundance δ^{18} O; 5) glucose at natural abundance δ^{13} C and 18 O-enriched water (atom fraction 97%). These treatments were selected in order to evaluate the effects of isotope addition on the density and isotopic composition of DNA. We assessed (I) the effect of ¹⁸O in the absence of supplemental glucose as the difference between treatment 2 and 1, (II) the effect of ¹³C in the presence of supplemental glucose as the difference between treatments 4 and 3, and (III) the effect of ¹⁸O with supplemental glucose as the difference between treatments 5 and 3. In each

143

144

145

146

147

148

149

150

151

152

153

154

155

156

157

158

159

160

161

162

163

164

typically included in SIP studies (24).

specific equations quantifying these comparisons are presented below. After the incubation, samples were frozen and stored at -40°C. DNA was extracted from approximately 0.5 g soil using a FastDNA® Spin Kit for Soil (MP Biomedicals, Santa Ana, CA, USA) following the manufacturer's directions. Extracted DNA was quantified using the Qubit® dsDNA High-Sensitivity Assay Kit and a Qubit® 2.0 Fluorometer (Invitrogen, Eugene, OR, USA). Density Centrifugation and Fraction Collection To separate DNA by density, 5 µg of DNA was added to approximately 2.6 mL of a saturated CsCl and gradient buffer (200 mM Tris, 200 mM KCl, 2 mM EDTA) solution in a 3.3 mL OptiSeal™ Ultracentrifuge tube (Beckman Coulter, Fullerton, CA, USA). The final density of the solution was 1.73 g cm⁻³. The samples were spun in an Optima™ MAX benchtop ultracentrifuge (Beckman Coulter, Fullerton, CA, USA) using a Beckman TLN-100 rotor at 127,000 x g for 72 hours at 18°C. After centrifugation, the density gradient was divided into fractions of 150 µL each using a fraction recovery system (Beckman Coulter Inc, Palo Alto, CA, USA). The density of each fraction was

subsequently measured with a Reichert AR200 digital refractometer (Reichert Analytical

Instruments, Depew, NY, USA). We did not include DNA standards of known GC

content in each ultracentrifuge tube. Such standards are traditionally included when

computing GC content based on density is the primary goal (e.g., 12, 23), but are not

case, these comparisons isolate the effect of the presence of an isotope tracer. The

DNA was separated from the CsCl solution using isopropanol precipitation, resuspended in 50 µL sterile deionized water, and quantified for each density fraction. We determined total number of bacterial 16S rRNA gene copies in each density fraction by qPCR using a pan-bacterial broad-coverage quantitative PCR technique (25). All fractions were analyzed in triplicate in 10 µl reactions that included 1 µl of DNA template and 9 µl of reaction mix containing 1.8 µM of forward (5'-CCTACGGGDGGCWGCA-3') and reverse (5'-GGACTACHVGGGTMTCTAATC-3') primers (bold letters denote degenerate bases), 225 nM of the TaqMan® minor groove-binding probe (6FAM) 5'-CAGCAGCCGCGGTA-3' (MGBNFQ), 1x Platinum® Quantitative PCR SuperMix-UDG (Life Technologies, Grand Island, NY), and molecular-grade water. Amplification and real-time fluorescence detection were performed on the 7900HT Real Time PCR System (Applied Biosystems). We provide the qPCR data for all density fractions in the supplementary online material.

178

180

181

182

183

184

185

186

165

166

167

168

169

170

171

172

173

174

175

176

177

179 Data analysis of total 16S rRNA gene copy number

> Based on the qPCR data, we produced a conventional SIP density curve by graphing the proportion of total 16S rRNA gene copies as a function of density, an approach often used to visualize the effect of isotope incorporation on the distribution of densities across the bacterial assemblage, delineating "heavy" and "light" regions for sequencing (9-11). We also calculated the average DNA density for each tube as a weighted average of the density of each fraction in which 16S rRNA gene copies were detected, weighted by the proportional abundance of total 16S rRNA gene copies measured in that fraction for each

187 tube. This provided an estimate of the average DNA density for each tube, enabling 188 testing via bootstrapping whether isotope addition increased the density of DNA.

189

190

191

192

193

194

195

196

197

198

199

200

201

202

203

204

205

206

207

Sequencing 16S rRNA genes

We sequenced the 16S rRNA gene in every density fraction that contained DNA (9-15 fractions per centrifuge tube) by a dual-indexing amplicon-based sequencing on the Illumina MiSeq (Illumina Inc, San Diego, CA, USA) following (26). For each density fraction, the 16S rRNA gene V3-V4 hypervariable region was amplified in 25 µl reactions that included 5 µl of gDNA in a 20 µl of reaction mix containing 12.5 µl Phusion High-Fidelity PCR Master Mix with HF Buffer (New England Biolabs Inc., Ipswich, MA, USA), 0.75 μl DMSO, and 1.75 μl of sterile water and 0.2 μM of each (5'-(5'-ACTCCTACGGGAGGCAGCAG-3') forward and reverse GGACTACHVGGGTWTC-TAAT-3') primers, each concatenated to a linker sequence, a 12bp barcode, and a "heterogeneity spacer" of 0-7bp in size. The following thermocyling condition was used: an initial denaturation at 98°C for 30s, followed by 30 cycles of denaturation at 98°C for 30s, annealing at 62°C for 30s, and amplification/ extension at 72°C for 30s. The resultant amplicons were normalized and pooled using the SequelPrep Normalization Kit (Life Technologies, Carlsbad, CA, USA), then purified using the AMPure XT beads (Beckman Coulter Genomics, Danvers, MA, USA) and sequenced in combination with ~20% of PhiX control library (v3) (Illumina) on 300bp paired-end MiSeq runs.

208

209

Data-analysis

Subsequent sequence processing and quality filtering were also performed as described in Fadrosh et al, 2014 (26). Each read was assigned to the original sample based on the 24bp dual-index barcode formed by concatenating the 12bp barcodes from each paired-end read. After trimming the primer sequences, the original V3-V4 amplicon was reconstituted by stitching the paired-end reads without preliminary quality filtering using FLASH (27), as FLASH includes error correction. We obtained 9,378,878 high-quality stitched reads that were subsequently processed at a median length of 410 bp.

217

218

219

220

221

222

223

224

210

211

212

213

214

215

216

The stitched reads were clustered using the uclust-based (28) open reference OTU picking protocol (29) described in QIIME (v1.8.0-dev) (30) against the Greengenes 13 8 reference database (31). Representative sequences for each OTU were chosen as the cluster centroid sequences. OTUs with representative sequences that could not be aligned with PyNAST and OTUs with a total count of less than 2 across all samples (i.e., singleton OTUs) were excluded from subsequent analyses, leaving a total of 76,710 OTUs composed of 9,127,632 reads.

225

226

227

228

229

230

231

232

All taxonomic assignments used throughout this study were generated by QIIME's uclust-consensus taxonomy assigner (default parameters, 32) against the Greengenes 13 8 97% reference OTUs (33). The taxonomic abundances for each sample-taxa combination using the uclust-consensus assigner were compared with taxonomic assignments made with the RDP classifier (confidence = 0.5, as recommended in 34) using a non-parametric Pearson correlation test with 999 iterations. For each sample-taxa combination, taxonomic abundances were compared for the two assignment methods

(i.e., using QIIME's compare_taxa_summaries.py script). The resulting p-values were significant (p<0.001) at all taxonomic levels, and the Pearson r-values were high (>0.96, Supplemental Material Table S1), indicating that the taxonomic profiles generated by the different methods were nearly identical. Analyses here focused on taxonomic classification to the level of genus, of which the uclust consensus assignment yielded a total of 790 genera. Genera included for analysis here were the 379 that occurred in all replicate tubes; these were also the most abundant taxa, representing 99.531% of the total 16S rRNA gene copies across the dataset. All QIIME commands used in this analysis are provided in Supplementary Information. All sequence data have been deposited at MG-RAST (35) project ID 14151.

243

244

245

246

247

248

249

250

251

252

253

254

255

233

234

235

236

237

238

239

240

241

242

Overview of quantitative taxon-specific isotope incorporation

In the following, we describe the calculations required to determine the isotopic composition of individual taxa after exposure to isotopically labeled substrates. In this approach, the taxon-specific density of DNA in the treatment with the isotopically labeled substrate is computed and compared to the density of DNA for the same taxon in the treatment with no added isotope tracer. For a particular element and isotope, the density of DNA will reach a maximum value when all atoms of that element in the DNA molecule are labeled with the isotope tracer. Smaller shifts in density reflect intermediate degrees of tracer incorporation; the scaling between density shift and isotope incorporation is linear after accounting for the effect of GC content on the elemental composition of DNA. The incorporation of the isotope tracer is expressed as atom fraction excess, which is the increase above natural abundance isotopic composition, and

ranges from a minimum of 0 to a maximum of 1 minus the natural abundance background for a given isotope-element combination. Variables, calculated quantities, and indices are defined in Table 1.

259

260

261

262

263

264

265

266

267

268

258

256

257

Calculating taxon-specific changes in density

Taxon specific changes in density caused by isotope incorporation were calculated as shown in equations 1-12, below. Calculations at the scale of individual density fractions (Eq. 1) and of individual replicate tubes (Eqs. 2, 3) were conducted for each density fraction and each tube independently. Other calculated quantities compared tubes with and without isotopes (Eqs. 4, and 10-12), where we used means across replicates to estimate the mean difference, and resampling with replacement (bootstrapping) to determine confidence intervals, as described below. In all cases, the independence of true replicates was preserved.

269

270

271

272

273

274

275

276

277

As described above, we determined the total number of 16S rRNA gene copies (f_k) using the universal 16S rRNA primer for qPCR for each fraction (k) in each replicate density gradient (j). Also as described above, we used sequencing to determine the proportional abundance of each taxon (i) within each density fraction (k), again for each replicate density gradient (j). This proportional abundance of each individual taxon within an individual density gradient from a particular replicate tube is abbreviated p_{ijk} . We calculated the total number of 16S rRNA gene copies per $\mu L(y_{ijk})$ for bacterial taxon i in density fraction k of replicate j as:

$$y_{ijk} = p_{ijk} \cdot f_{jk} \tag{1}$$

279 The total number of 16S rRNA gene copies (y_{ij}) for bacterial taxon i in replicate j is 280 summed across all *K* density fractions:

$$y_{ij} = \sum_{k=1}^{K} y_{ijk}$$
 (2)

282

283 The density (W_{ii}) for bacterial taxon i of replicate j was computed as a weighted average, 284 summing across all K density fractions the density (x_{ik}) of each individual fraction times 285 the total number of 16S rRNA gene copies (y_{iik}) in that fraction expressed as a proportion 286 of the total 16S rRNA gene copies (y_{ij}) for taxon i in replicate j:

$$W_{ij} = \sum_{k=1}^{K} x_{jk} \cdot \left(\frac{y_{ijk}}{y_{ij}}\right)$$
(3)

288 For a given taxon, we calculated the difference in density caused by isotope incorporation

289 (Z_i) :

291

292

293

294

295

296

$$Z_{i} = W_{LABi} - W_{LIGHTi} \tag{4}$$

where W_{LABi} is the mean, across all replicates, of the isotope-enriched treatment (labeled, LAB; n=3) and W_{LIGHTi} is the mean, across all replicates, of the unlabeled treatment (unlabeled, LIGHT; n=6). Because our experiment had multiple treatments without heavy isotopes, we included data from all replicate tubes in those unlabeled treatments (i.e., unlabeled treatments with and without added carbon; n=6) to estimate the unlabeled average density (W_{LIGHTi}) for each taxon i.

297

298

Calculating taxon-specific GC content and molecular weight

300

301

302

303

304

306

318

320

We calculated the GC content (G_i) of each bacterial taxon using the mean density for the unlabeled (W_{LIGHTi}) treatments (n=6). We derived the relationship between GC content and buoyant density using DNA from pure cultures of three microbial species with known but strongly differing GC content (see below). For these cultures, the linear relationship between GC content (G_i , expressed as a proportion) and unlabeled buoyant density (W_{LIGHTi}) on a CsCl gradient was:

$$G_i = \frac{1}{0.083506} \cdot (W_{LIGHTi} - 1.646057) \tag{5}$$

This relationship differs from the established relationship between GC content and

307 density (12). As noted above, our method of determining density relied on direct 308 measurements of refraction on individual density fractions, as is the typical practice for 309 SIP studies (24). Possibly, including DNA standards of known GC content in each 310 ultracentrifuge would yield results more consistent with the established relationship. 311 Practitioners should include specific measures to calibrate their laboratory techniques to 312 this relationship. 313 The natural abundance molecular weight of DNA is a function of GC content, based on 314 the atomic composition of the four DNA nucleotides. Single stranded DNA made of pure adenine (A) and thymine (T) has an average molecular weight of 307.691 g mol⁻¹. The 315 316 corresponding average molecular weight for DNA comprising only guanine (G) and cytosine (C) is 308.187 g mol⁻¹. When GC content is known, the average molecular 317

$$M_{LIGHTi} = 0.496G_i + 307.691 \tag{6}$$

321 Percent change in molecular weight associated with isotope incorporation

weight of a single strand of DNA can be calculated using:

323

324

325

326

327

328

329

330

There are 12 oxygen atoms per DNA nucleotide pair, regardless of GC content: there are 6 for each G and C, and 7 for T, 5 for A). These atoms contain ¹⁸O at natural abundance, which we assume to be 0.002000429 atom fraction for ¹⁸O (36). The maximum labeling is achieved when all oxygen atoms are replaced by ¹⁸O. Therefore, given the molecular weight of each additional neutron (1.008665 g mol⁻¹; 37), the maximal increase in molecular weight (corresponding to 1 atom fraction ¹⁸O, or 100% atom percent ¹⁸O) is 12.07747 g mol⁻¹. The theoretical maximum molecular weight ($M_{HEAVYMAXi}$) of fully ¹⁸Olabeled DNA for taxon i is then: $M_{HEAVYMAXi} = 12.07747 + M_{LIGHTi}$

$$M_{HEAVYMAXi} = 12.07/47 + M_{LIGHTi}$$
 (7)

331 In contrast, the number of carbon atoms per DNA nucleotide varies with GC content.

332 There are 10 carbon atoms in G, A, and T, but only 9 in C. The average number of

333 carbon atoms per DNA nucleotide ($H_{CARBONi}$) for taxon i can therefore be expressed as:

$$H_{CARBONi} = -0.5G_i + 10 \tag{8}$$

We assume these atoms are ¹³C-labeled at natural abundance (0.01111233 atom fraction 335

¹³C; (36)). The maximal labeling is achieved when all carbon atoms are replaced by ¹³C. 336

Complete replacement of carbon atoms with ¹³C increases the molecular weight by 337

9.974564 g mol⁻¹ for G, A, and T, and by 8.977107 g mol⁻¹ for C. Using equation 8, the 338

339 theoretical maximum molecular weight ($M_{HEAVYMAXi}$) of fully ¹³C-labeled DNA can be

340 calculated as follows, with GC content (G_i) expressed as a proportion:

$$M_{HEAVYMAXi} = -0.4987282Gi + 9.974564 + M_{LIGHTi}$$
(9)

342 Calculating isotope enrichment from density shifts 343 We calculated the proportional increase in density (Z_i) relative to the density of the 344 unlabeled treatments (W_{LIGHTi}), and calculated molecular weight of DNA for taxon i in 345 the labeled treatment (M_{LABi}) as:

$$M_{LABi} = \left(\frac{Z_i}{W_{LIGHTi}} + 1\right) \cdot M_{LIGHTi}$$
(10)

The atom fraction excess of 18 O for taxon i ($A_{OXYGENi}$), accounting for the background 347

fractional abundance of ¹⁸O (0.002000429 (36)) is then calculated as: 348

349
$$A_{OXYGENi} = \frac{M_{LABi} - M_{LIGHTi}}{M_{HEAVYMAXi} - M_{LIGHTi}} \cdot (1 - 0.002000429)$$
 (11)

. We used the results from a pure culture study with E. coli, grown with variable ¹⁸O-350

enriched water (natural abundance, 5, 25, 50, and 70% atom fraction ¹⁸O; see below) to 351

compare to the theoretical calculations of atom fraction excess ¹⁸O derived above. 352

Similarly, the atom fraction excess 13 C for taxon i ($A_{CARBONi}$) accounting for the 353

background fractional abundance of ¹³C (0.01111233, 36), is calculated as: 354

355
$$A_{CARBONi} = \frac{M_{LABi} - M_{LIGHTi}}{M_{HEAVYMAXi} - M_{LIGHTi}} \cdot (1 - 0.01111233)$$
 (12)

356 Pure culture studies

357 To verify the predicted relationship between increased density and atom fraction excess

358 we conducted experiments with a pure Escherichia coli culture. E. coli (strain HB101,

359 GC content 50.8%) was shaken at 100 rpm, 37 °C for 8 h in Luria-Bertani (LB) broth that

was prepared with a mixture of natural abundance and ¹⁸O-water to achieve five ¹⁸O-360

enrichment levels (natural abundance, 5, 25, 50, and 70% atom fraction ¹⁸O). Genomic 361

362 DNA was extracted in triplicate using PowerLyzer UltraClean Microbial DNA Isolation

363 Kit according to the manufacturer's instructions (MO BIO Laboratories, Inc., Carlsbad,

composition of E. coli DNA and its density.

364 CA). We also grew pure cultures of two additional strains of bacteria selected for low GC 365 content (Staphylococcus epidermidis, ATTC# 49461, 32.1%) and high GC content 366 (Micrococcus leuteus, ATTC# 49732, 73%). S. epidermidis was grown for 24 h on Brain Heart Infusion Agar at 37 °C, and M. leuteus was grown with LB agar at 23 °C. These 367 cultures were grown with substrates and water at natural abundance stable isotope 368 369 composition. 370 371 For each culture, genomic DNA was extracted in triplicate. Approximately 800 ng of 372 each DNA extract was used for isopycnic centrifugation, density quantification, and DNA isotope analysis. The ¹⁸O composition of the E. coli DNA was determined with a 373 374 PyroCube (Elementar Analysensysteme GmbH, Hanau, Germany) interfaced to a PDZ 375 Europa 20-20 isotope ratio mass spectrometer (Sercon Ltd., Cheshire, UK) at the UC 376 Davis Stable Isotope Facility (Davis, CA). Samples were prepared by diluting the E. coli 377 DNA with natural abundance salmon sperm DNA to achieve enrichment levels below 100 % δ^{18} O for isotope analysis. Densities of DNA from the cultures grown at natural 378 379 abundance isotope composition were used to determine the relationship between the density of DNA and its GC content, yielding the relationship described in Eq. 5 (r^2 = 380 381 0.912, P < 0.001). 382 383 Statistical analysis We used linear regression to examine the relationships between ¹⁸O-H₂O composition of 384 the growth medium and the ¹⁸O composition of E. coli DNA, and also between the ¹⁸O 385

388

389

390

391

392

393

394

395

396

397

398

399

400

401

402

403

404

405

406

407

408

409

Following the equations above, we computed the difference in densities, Z_i , between treatments with and without isotope tracers, and the corresponding values of isotope composition, A_{OXYGEN} and A_{CARBON}. Each calculated quantity was determined for each replicate sample. We then used bootstrap resampling (with replacement, 1000 iterations) of replicates within each treatment to estimate taxon-specific 90% confidence intervals for the change in density (Eq. 4) and the corresponding value of atom fraction excess isotope composition (Eq. 11 for oxygen, Eq. 12 for carbon). For each bootstrap iteration, three samples (with replacement) were drawn from the isotope added treatment, and six samples were drawn from the no-isotope controls. All calculations were performed in R (38).Density fractionation separates organisms according to GC content (12) as well as isotope incorporation, so traditional SIP may be biased toward identifying high-GC content organisms as growing or utilizing a substrate (39, 40). To test whether qSIP exhibited any such bias, we used density without isotope addition as a proxy for GC content, and tested whether the densities of organisms identified as assimilating (90% confidence intervals did not include 0 for A_{CARBON} or A_{OXYGEN}) differed in density from organisms where assimilation was not detected. Our focus was on the magnitude of variation in Z_i , A_{OXYGEN} , and A_{CARBON} , because the goal of our work was to establish a means to discern from SIP experiments quantitative

estimates of isotope tracer uptake. These values lie along a continuum from no uptake to

complete isotope replacement, and our approach estimates the values and places

confidence limits on those estimates. We did not use null hypothesis significance testing for assessing density shifts and isotope tracer uptake, because our priority was on estimation rather than determining statistical significance. For this reason, we selected bootstrap resampling rather than, for example, t-tests or ANOVAs. Parametric tests could of course be applied in future applications of this technique, and may be appropriate, for example, for statistical comparisons of treatments postulated to alter isotope tracer uptake. In such cases, correcting for multiple comparisons may be appropriate, depending on the nature of the question and the balance between type I and type II error rates. We note that, in typical SIP experiments, an organism is considered to be growing or utilizing a substrate if it exhibits a change in relative abundance when comparing the heavy fraction of the labeled versus control (e.g., 10) or comparing the heavy fraction versus the light fraction (e.g., 41), yet assessments of variation in these estimates are not typically presented. Our approach assesses both the quantitative values of isotope uptake and the variation associated with those estimates.

424

410

411

412

413

414

415

416

417

418

419

420

421

422

423

D		1	4
к	es	ш	TS

426

427

428

429

430

431

432

433

434

435

436

In the pure culture experiments, the ¹⁸O composition of *E. coli* DNA was strongly related to the ¹⁸O composition of water in the growth medium, supporting the notion that oxygen from water is quantitatively incorporated into the DNA of growing organisms (P<0.001, $r^2 = 0.976$, Figure 2A). The slope of the relationship, 0.334 ± 0.017 (n=15), indicates that 33% of oxygen in E. coli DNA was derived from water. The shift in density of E. coli DNA with ¹⁸O incorporation matched well the theoretical prediction of the model of isotope substitution in the DNA molecule (Equations 10 and 11, Figure 2B). These results confirm that ultracentrifugation in CsCl can serve as a quantitative mass separation procedure, resolving variation in isotope tracer incorporation into DNA. These results also support our model of the relationship between the density of nucleic acids and isotopic substitution in the DNA molecule.

437

438

439

440

441

442

443

444

445

446

447

In soil incubations, DNA density averaged across the entire community tended to increase in response to isotope addition (Figure 3). Addition of ¹³C-glucose (Figure 3A) increased the density of DNA by 0.0043 g cm⁻³, but the 90% confidence interval for this increase overlapped zero (-0.002 to 0.0091 g cm⁻³). Addition of ¹⁸O-water (Figure 3B) caused a similar increase in density, 0.0041 g cm⁻³, but the 90% confidence interval for this increase also overlapped zero, spanning -0.0011 to 0.0090 g cm⁻³. The incubations receiving ¹⁸O-water and supplemental glucose (natural abundance isotope composition) exhibited the largest increase in average DNA density, 0.0090 g cm⁻³, and in this case the 90% confidence limit did not overlap zero (0.0065 to 0.0125 g cm⁻³). These comparisons estimate the change in density of DNA fragments encoding the 16S rRNA gene across all

taxa considered together. Figure 3 also illustrates the density distributions often used in SIP experiments to visualize the qualitative cutoff between labeled and unlabeled regions suitable for sequencing.

451

452

453

454

455

456

457

458

459

460

461

462

463

464

465

466

467

468

469

470

448

449

450

Sequencing all fractions allowed visualizing analogous density distributions for individual taxa. Figure 4 shows three taxa to illustrate the concept, showing graphically the manner in which the density of labeled (W_{LABi}) and unlabeled (W_{LIGHTi}) DNA is calculated for each taxon (equation 3). For example, the density of an unidentified genus in the family *Micrococcaceae* did not change with ¹⁸O-water addition in the absence of supplemental glucose. For this taxon, the shift in density (Z) due to ¹⁸O incorporation was -0.0002 g cm⁻³, with the 90% confidence interval spanning -0.0046 to 0.0049 g cm⁻³ (Figure 4A). The shift in density due to ¹⁸O-incorporation increased when unlabeled glucose was also added (Figure 4B, $Z = 0.0169 \text{ g cm}^{-3}$, 90% CI, 0.0146 to 0.0194 g cm⁻³). This bacterial taxon was therefore not incorporating the ¹⁸O tracer in unamended soil, but synthesized new DNA using ¹⁸O derived from H₂O in response to glucose addition. The DNA of an unidentified genus in the family Pseudonocardiaceae similarly exhibited no change in density in the absence of supplemental glucose ($Z = 0.0005 \text{ g cm}^{-3}$, -0.0033 to 0.0045 g cm^{-3}), and exhibited only a slight increase in response to glucose addition (Z = 0.0040 g cm⁻³, 0.0015 to 0.0070 g cm⁻³, Figure 4C & D). By contrast, the density of DNA in a member of the genus Herpetosiphonales increased in soil without any supplemental glucose ($Z = 0.0124 \text{ g cm}^{-3}$, 90% CI, 0.0105 to 0.0143 g cm⁻³, Figure 4E), but the density did not further increase in response to the addition of glucose ($Z = 0.0110 \text{ g cm}^{-3}$, 90% CI, 0.0088 to 0.0133 g cm⁻³, Figure 4F). These results show that, by dividing the density

gradient into multiple fractions and sequencing each separately, one can determine changes in the density of DNA for individual taxa caused by the assimilation of stable isotope tracers.

474

475

476

477

478

479

480

481

482

483

484

471

472

473

The taxon-specific shifts in average density associated with incorporation of the heavy isotope (Figure 5) translate directly to quantitative variation in isotope composition, expressed here as atom fraction excess 18 O (A_{OXYGEN} , Figure 5A & B) and 13 C (A_{CARBON} , Figure 5C). The detection limit for a shift in density is the median change in density required to shift the lower bound of the bootstrapped 90% confidence limit above zero. As constrained by our sampling design, these values were 0.0037 g cm⁻³ for ¹⁸O, and 0.0044 g cm⁻³ for ¹³C, changes that correspond to 0.056 atom fraction excess ¹⁸O and 0.081 atom fraction excess ¹³C. No taxon exhibited a detectable decline in density in response to isotope addition (i.e., a negative mean density shift with confidence interval that did not include zero).

485

486

487

488

489

490

491

492

493

More than half of the bacterial genera (209) did not exhibit any detectable excess ¹⁸O enrichment under control conditions without added glucose; in other words, the lower bound of the confidence intervals for these genera overlapped zero (Figure 5A). Of the 170 taxa that did exhibit detectable ¹⁸O enrichment without added glucose, the corresponding values of atom fraction excess ¹⁸O ranged from 0.047 (90% confidence interval, 0.001 to 0.100) in a member of the genus, *Lentzea*, to 0.354 (CI, 0.248 to 0.449) in an unidentified representative of the candidate bacterial phylum, OD1. With added glucose, 351 of the 379 taxa exhibited positive atom fraction excess ¹⁸O (90% CIs did not overlap zero), averaging 0.147 (Figure 5B), with a minimum of 0.036 (CI, 0.004 to 0.064) in an unidentified genus of the family Ktedonobacteracea, and a maximum of 0.365 (CI, 0.282 to 0.449) in an unidentified genus within the class AT12OctB3 of the phylum, Bacteroidetes. Bacterial taxa in this soil varied in atom fraction excess ¹⁸O under control conditions and in response to added glucose (Figure 5A & B). Atom fraction excess ¹³C reflects direct assimilation of C from the added glucose (Figure 5C), and ranged from no detectable enrichment among 215 of the 379 genera, to over half of the carbon atoms comprising ¹³C in the DNA of a member of the *Micrococcaceae* (0.525, CI 0.458 to 0.592).

503

504

505

506

507

508

509

494

495

496

497

498

499

500

501

502

GC Bias

There was no evidence of GC bias in qSIP. There were negligible differences in densities between organisms exhibiting tracer assimilation and those not exhibiting tracer assimilation (Table 2). Inferred GC contents averaged 52.3% (CI 44.6% to 57.3%) for organisms exhibiting tracer assimilation, very close to the average of 52.8% inferred GC content for taxa for which assimilation was not detected (CI 45.1% to 58.2%).

510

511

512

513

514

515

516

Soil Incubations: multi-element quantitative stable isotope probing

There was a strong positive relationship between increased atom fraction excess ¹⁸O in response to glucose addition and the direct utilization of glucose-derived C (atom fraction excess ¹³C; Figure 6; r²=0.51, P<0.001). The expected relationship (solid line in Figure 6) reflects the case where glucose is the sole C source, and thus there should be an 0.33 atom fraction excess increase in ¹⁸O for each 1 atom fraction excess increase in ¹³C,

- based on our finding that 33% of the oxygen molecules in DNA are derived from water 517
- (Figure 2). For many taxa, the increase in atom fraction excess ¹⁸O in response to added 518
- 519 glucose exceeded the expected amount (solid line in Figure 6).

Discussion

We demonstrate that stable isotope probing of bacterial assemblages in natural environments can yield quantitative information about the assimilation of isotope tracers into bacterial DNA with fine taxonomic resolution. This work establishes a framework for coupling quantitative interpretation of stable isotope tracer experiments with microbial diversity, a coupling essential for understanding how to represent microbial diversity in biogeochemical models.

527

528

529

530

531

532

533

534

535

536

537

538

539

540

541

542

520

521

522

523

524

525

526

The shifts in density we could detect using qSIP (0.0034 to 0.0042 g cm⁻³, Figure 5) are nearly an order of magnitude smaller than those typically used to resolve the assimilation of stable isotopes into newly synthesized DNA using conventional SIP, in which "light" and "heavy" density fractions often differ by 0.03 g cm⁻³ (14, 42) or more (13, 24, 43). For ¹³C, the minimum required change in density for SIP has been estimated to be 0.01 g cm⁻³, corresponding to 0.2 atom fraction excess (7). The approach presented here achieves higher resolution by accounting for taxonomic differences in the density of DNA caused by natural variation in GC content. It may be possible to improve the resolution we achieved. We collected fractions in discrete density increments of 0.0036 g cm⁻³ (average difference in density between adjacent fractions), setting a limit on the changes in density we could detect. This difference in density between adjacent fractions we collected is comparable to the density shifts of bacterial taxa that we could resolve: the mean density shift required for the lower confidence limit to exceed zero was, on average, 0.0034 g cm⁻³ for ¹⁸O and 0.0042 g cm⁻³ for ¹³C. Thus, it is possible that separation of the nucleic acids into finer density fractions will afford higher precision in

the estimates of stable isotope composition. Furthermore, our sample size was quite low; higher replication would achieve finer resolution. Nevertheless, the finding that no taxon exhibited a detectable decline in density in response to isotope addition is encouraging. Such a result would be illogical because isotope tracer uptake cannot be negative, but could arise from large random variation (natural and measurement error) and low sample size. The absence here of such negative confidence intervals indicates that our bootstrapping application to qSIP is not particularly subject to false positive inference.

550

551

552

553

554

555

556

557

558

559

560

561

562

543

544

545

546

547

548

549

The resolution achieved by sequencing individual density fractions, though an improvement over traditional SIP, is still very coarse compared to the resolution achieved with isotope ratio mass spectrometry. Detecting differences between taxa with quantitative stable isotope probing (~0.05 atom fraction excess) is four orders of magnitude less precise than that achieved with gas isotope ratio analysis of bulk organic matter in continuous flow, where differences of 0.000005 atom fraction excess or better (<0.5%) can be resolved (44). Isopycnic centrifugation to quantify isotope composition is also less precise than compound specific analysis of biomarkers, for example, of ¹³C in fatty acids, where resolution of 0.00002 atom fraction excess (or 2%) is typical (45-47). Coupling stable isotope tracing with Nano-scale secondary ion mass spectrometry (Nano-SIMS) and microarrays, a coupling called Chip-SIP (48), can resolve 0.005 atom fraction excess for ¹⁵N and 0.001 for ¹³C (49), considerably more precise than qSIP.

563

564

565

qSIP has advantages in taxonomic resolution over these other techniques. For compound specific biomarkers, specific fatty acids serve as biomarkers for up to a dozen groups of microorganisms, taxonomic resolution much coarser than that afforded by qSIP. Chip-SIP requires nucleic acid probes, necessitating deciding a priori what sequences to collect for isotopic analysis, and preparing microarrays implanted with those sequences prior to the isotope addition. For this reason, in Chip-SIP the taxonomic resolution in the isotope fluxes is influenced by information gathered without knowledge of which taxa are biogeochemically important. One advantage of qSIP is that sequencing occurs after isotope enrichment, enabling quantitative exploration of the biodiversity involved in biogeochemistry, without having to decide where to focus a priori. Furthermore, the taxonomic resolution possible with a microarray is limited by probe specificity and fidelity, whereas the resolution afforded by qSIP is very high, equivalent to the resolution of sequencing technology applied to the density fractions. Chip-SIP also requires access to a Nano-SIMS, expensive and technically challenging, limiting its wide adoption in the field.

579

580

581

582

583

584

585

586

587

588

566

567

568

569

570

571

572

573

574

575

576

577

578

Other approaches used to link element fluxes to microbial taxa are limited to target organisms, such as fluorescent in situ hybridization (FISH) coupled with SIMS (50), or halogen in situ-hybridization-SIMS (51). Bromodeoxyuridine (BrdU) uptake has been proposed as a universal technique for identifying growing organisms (52) and their responses to environmental perturbations (53). However, there is up to 10-fold variation among taxa in the conversion between BrdU uptake and growth, unrelated to taxonomic affiliation, a bias calling into question the quantitative universality of this technique (54). Compared to these other techniques, qSIP can assess quantitatively the entire microbial assemblage at fine taxonomic resolution, a solid foundation for exploring quantitatively

the relationships between microbial biodiversity and the biogeochemistry known to be microbial.

591

592

593

594

595

596

597

598

599

600

601

602

603

604

605

606

607

608

609

610

611

589

590

Our finding that many bacterial taxa did not exhibit any increase in ¹⁸O content under control conditions (Figure 5A) is consistent with the notion that a portion of the soil microbial biomass is not growing and may be metabolically inactive (55). The increase in atom fraction ¹⁸O and ¹³C with added glucose indicates that glucose addition stimulates bacterial growth, not just respiration. The breadth of taxa that exhibited a positive response to glucose addition is consistent with glucose being a widely utilized substrate (56), though there are two other possible mechanisms. First, over the 7-day duration of the incubation period, glucose will be assimilated by cells that then died, releasing labeled cellular constituents available to the rest of the microbial community (57). We cannot distinguish between direct utilization of the added glucose and utilization of labeled cellular constituents produced by another organism. This applies equally to the ¹⁸O-labeled and ¹³C-labeled assemblages. Second, ¹⁸O-water is a universal tracer for DNA synthesis, not necessarily tied to any particular carbon source (58, 59). The observed increase in atom fraction excess ¹⁸O includes growth stimulation caused by the carbon contained in the added glucose, along with the growth stimulation caused by increased rates of utilization of other carbon sources. In contrast, atom fraction excess ¹³C in response to ¹³C-glucose addition traces the incorporation of carbon atoms from glucose (or derived from glucose via other metabolites as discussed above) into newly synthesized DNA (Figure 5C). This is expected, because glucose addition stimulates growth and DNA synthesis (60, 61). In summary, the effect of added glucose was

apparent as: (1) an overall stimulation of growth, independent of the specific carbon substrate, and (2) as a stimulation of growth that relied directly on glucose-derived carbon.

615

616

617

618

619

620

621

622

623

624

612

613

614

The combination of ¹⁸O and ¹³C tracers enabled quantitative partitioning of these direct and indirect effects, based on the deviation in the data from the expected relationship between ¹⁸O and ¹³C enrichment for organisms utilizing glucose as a sole carbon source (solid line, Figure 6). One explanation for this deviation is that most taxa derive more than 33% of the oxygen in DNA from environmental water. Quantitative variation in the contribution of water to oxygen in DNA could occur, for example, due to the variation in the oxidation state of the carbon substrate (e.g., lipids versus carbohydrates), though to our knowledge this variation is not known. Given the universality of the mechanism of DNA replication, it is unlikely that taxa vary widely in the contribution of water to oxygen, at least when grown on a common substrate.

626

627

628

629

630

631

632

633

634

625

A more parsimonious explanation of the deviation we observed is that it represents utilization of C sources other than glucose for growth. In other words, the added glucose stimulated the utilization of native soil C as a growth substrate. This points to the potential for quantitative stable isotope probing to test hypotheses regarding microbial diversity in the commonly observed phenomenon where the addition of simple C substrates to soil alters the mineralization of native soil C (16). This so-called "priming effect" is common and quantitatively significant (16), but remains mechanistically inscrutable. In past priming studies employing ¹³C-SIP, some components of the

microbial community were found to utilize as growth substrates the ¹³C-labeled compounds added to initiate priming, though inferences about the organisms responsible for priming - i.e., degrading native soil organic matter - were weak, because no independent marker could validate their activity (62-64). Combining isotope tracers (using both ¹³C and ¹⁸O) can help by distinguishing microorganisms that respond to the original substrate pulse from those that respond indirectly by degrading soil organic matter (11), an approach useful for testing hypotheses about which groups of microorganisms contribute to priming, qSIP advances this one step further, by enabling quantitative comparisons of microorganisms' utilization of the added substrate and of soil organic matter for growth. Future analyses combining qSIP with system-level C fluxes would support stronger inferences about the role of specific microorganisms in the priming effect. The analysis presented here suggests that some microorganisms respond to glucose addition by enhancing their rates of utilization of native soil carbon, enabling additional biosynthesis (Figure 6). More generally, the taxonomic diversity of responses we observed highlights the potential for this technique to provide insight into the population and community ecology behind biogeochemical phenomena involving such indirect effects (e.g., 16, 17).

652

653

654

655

656

657

635

636

637

638

639

640

641

642

643

644

645

646

647

648

649

650

651

Quantifying isotope composition is the first step in determining the rate of substrate utilization in isotope tracer experiments, and the foundation for comparing rates of substrate utilization and element fluxes among different taxa in intact microbial communities. This work advances a quantitative approach to stable isotope probing in order to elucidate taxon-specific processes that drive element cycling in intact

communities, bringing to microbial ecology the power of stable isotopes to quantify rates of element fluxes into and through organisms (65, 66). Like Chip-SIP (48, 67), qSIP provides a means to quantify the ecology of organisms about which we know little more than the genetic fragment used to identify their unique place on the tree of life. These approaches lay the groundwork for a quantitative understanding of microbial ecosystems, including the types of ecological interactions previously described among macroorganisms that influence ecosystem processes. Quantitative stable isotope probing adds to the suite of tools that facilitate interpretation of stable isotope tracer experiments in microbial communities, probing the quantitative significance of microbial taxa for biogeochemical cycles in nature.

668

669

670

671

658

659

660

661

662

663

664

665

666

667

Acknowledgements. This research was supported by grants from the National Science Foundation (EAR-1124078 and DEB-1321792) and the Department of Energy's

Biological Systems Science Division, Program in Genomic Science.

672

673 References 674 1. Jenny H. 1941. Factors of Soil Formation: A System of Quantitative Pedology. 675 Dover Publications, New York. 676 2. Vitousek PM. 1990. Biological Invasions and Ecosystem Processes - Towards an 677 Integration of Population and Ecosystem Studies. Oikos 57:7-13. 678 3. Pace NR. 1997. A molecular view of microbial diversity and the biosphere. 679 Science 276:734-740. 680 4. Amann RI, Ludwig W, Schleifer KH. 1995. Phylogenetic Identification and in 681 situ Detection of Individual Microbial Cells without Cultivation. Microbiological 682 Reviews **59:**143-169. 683 5. Muyzer G, Dewaal EC, Uitterlinden AG. 1993. Profiling of Complex 684 microbial-Populations by Denaturing Gradient Gel-Electrophoresis Analysis of 685 Polymerase Chain Reaction-Amplified Genes Coding for 16S Ribosomal-RNA. 686 Applied and Environmental Microbiology **59:**695-700. 687 6. Roesch LF, Fulthorpe RR, Riva A, Casella G, Hadwin AKM, Kent AD, 688 Daroub SH, Camargo FAO, Farmerie WG, Triplett EW. 2007. 689 Pyrosequencing enumerates and contrasts soil microbial diversity. Isme Journal 690 1:283-290. 691 7. Radajewski S, Ineson P, Parekh NR, Murrell JC. 2000. Stable-isotope probing 692 as a tool in microbial ecology. Nature **403**:646-649. 693 8. Hutchens E, Radajewski S, Dumont MG, McDonald IR, Murrell JC. 2004. 694 Analysis of methanotrophic bacteria in Movile Cave by stable isotope probing.

Environmental Microbiology **6:**111-120.

718

16.

696 9. Sharp CE, Martinez-Lorenzo A, Brady AL, Grasby SE, Dunfield PF. 2014. 697 Methanotrophic bacteria in warm geothermal spring sediments identified using 698 stable-isotope probing. FEMS microbiology ecology **90:**92-102. 699 10. Schwartz E, Van Horn DJ, Buelow HN, Okie JG, Gooseff MN, Barrett JE, 700 **Takacs-Vesbach CD.** 2014. Characterization of growing bacterial populations in 701 McMurdo Dry Valley soils through stable isotope probing with O-18-water. Fems 702 Microbiology Ecology 89:415-425. 703 11. Mau RL, Liu CM, Aziz M, Schwartz E, Dijkstra P, Marks JC, Price LB, 704 **Keim P, Hungate BA.** 2014. Linking soil bacterial diversity and soil carbon 705 stability. The ISME Journal 9:1477-1480. 706 12. Schildkraut CL. 1962. Determination of Base Composition of Deoxyribonucleic 707 Acid from its Buoyant Denstiy in CsCl. Journal of Molecular Biology 4:430-443. 708 13. Schmidt O, Horn MA, Kolb S, Drake HL. 2015. Temperature impacts 709 differentially on the methanogenic food web of cellulose-supplemented peatland 710 soil. Environmental microbiology 17: 720-734. 711 14. Aanderud ZT, Jones SE, Fierer N, Lennon JT. 2015. Resuscitation of the rare 712 boisphere contributes to pulses of ecosystem activity. Frontiers in Microbiology 713 **6**: 24. 714 15. **Jayamani I, Cupples AM.** 2015. Stable Isotope Probing and High-Throughput 715 Sequencing Implicate Xanthomonadaceae and Rhodocyclaceae in Ethylbenzene 716 Degradation. Environmental Engineering Science 32:240-249.

Kuzyakov Y, Friedel JK, Stahr K. 2000. Review of mechanisms and

quantification of priming effects. Soil Biology & Biochemistry 32:1485-1498.

740

24.

719 17. Bingeman CW, Varner JE, Martin WP. 1953. The effect of the addition of 720 organic materials on the decomposition of an organic soil. Soil Science Society of 721 America Proceedings 17:34-38. 722 18. **Lohnis.** 1926. Nitrogen availability of green manures. Soil Science Society of 723 America Journal 22:171-177. 724 19. Broadbent FE. 1948. Nitrogen release and carbon loss from soil organic matter 725 during decomposition of added plant residues. Proceedings Soil Science Society 726 of America, 1947 12:246-249. 727 Broadbent FE, Bartholomew WV. 1949. The effect of quantity of plant material 20. 728 added to soil on its rate of decomposition. Proceedings Soil Science Society of 729 America, 1948 13:271-274. 730 21. **Kuzyakov Y.** 2002. Review: Factors affecting rhizosphere priming effects. 731 Journal of Plant Nutrition and Soil Science-Zeitschrift Fur Pflanzenernahrung 732 Und Bodenkunde 165:382-396. 733 22. Blagodatskaya E, Kuzyakov Y. 2008. Mechanisms of real and apparent priming 734 effects and their dependence on soil microbial biomass and community structure: 735 critical review. Biology and Fertility of Soils 45:115-131. 736 23. Mesbah NM, Whitman WB, Mesbah M. 2011. Determination of the G plus C 737 Content of Prokaryotes, p 299-324. In Rainey F, Oren A (ed), Methods in 738 Microbiology, Vol 38: Taxonomy of Prokaryotes, vol 38.

Neufeld JD, Vohra J, Dumont MG, Lueders T, Manefield M, Friedrich MW,

Murrell JC. 2007. DNA stable-isotope probing. Nature Protocols 2:860-866.

763

31.

741 25. Liu CM, Aziz M, Kachur S, Hsueh P-R, Huang Y-T, Keim P, Price LB. 2012. 742 BactQuant: An enhanced broad-coverage bacterial quantitative real-time PCR 743 assay. Bmc Microbiology 12:56. 744 Fadrosh DW, Ma B, Gajer P, Sengamalay N, Ott S, Brotman RM, Ravel J. 26. 745 2014. An improved dual-indexing approach for multiplexed 16S rRNA gene 746 sequencing on the Illumina MiSeq platform. Microbiome 2:6. 747 27. Magoc T, Salzberg SL. 2011. FLASH: fast length adjustment of short reads to 748 improve genome assemblies. Bioinformatics 27:2957-2963. 749 28. Edgar RC. 2010. Search and clustering orders of magnitude faster than BLAST. 750 Bioinformatics **26:**2460-2461. 751 29. Rideout JR, He Y, Navas-Molina JA, Walters WA, Ursell LK, Gibbons SM, 752 Chase J, McDonald D, Gonzalez A, Robbins-Pianka A, Clemente JC, Gilbert 753 JA, Huse SM, Zhou HW, Knight R, Caporaso JG. 2014. Subsampled open-754 reference clustering creates consistent, comprehensive OTU definitions and scales 755 to billions of sequences. PeerJ 2:e545. 756 30. Caporaso JG, Kuczynski J, Stombaugh J, Bittinger K, Bushman FD, Costello 757 EK, Fierer N, Pena AG, Goodrich JK, Gordon JI, Huttley GA, Kelley ST, 758 Knights D, Koenig JE, Ley RE, Lozupone CA, McDonald D, Muegge BD, 759 Pirrung M, Reeder J, Sevinsky JR, Turnbaugh PJ, Walters WA, Widmann 760 J, Yatsunenko T, Zaneveld J, Knight R. 2010. QIIME allows analysis of high-761 throughput community sequencing data. Nat Methods 7:335-336.

McDonald D, Price MN, Goodrich J, Nawrocki EP, DeSantis TZ, Probst A,

Andersen GL, Knight R, Hugenholtz P. 2012. An improved Greengenes

786

2015.

764 taxonomy with explicit ranks for ecological and evolutionary analyses of bacteria and archaea. ISME J 6:610-618. 765 766 32. Bokulich NA, Rideout JR, Kopylova E, Bolyen E, Patnode J, Ellett Z, 767 McDonald D, Wolfe B, Maurice CF, Dutton RJ, Turnbaugh PJ, Knight R, 768 Caporaso JG. 2015. A standardized, extensible framework for optimizing 769 classification improves marker-gene taxonomic assignments. PeerJ PrePrints. 770 33. McDonald D, Price MN, Goodrich J, Nawrocki EP, DeSantis TZ, Probst A, 771 Andersen GL, Knight R, Hugenholtz P. 2012. An improved Greengenes 772 taxonomy with explicit ranks for ecological and evolutionary analyses of bacteria 773 and archaea. ISME J 6:610-618. 774 34. Claesson MJ, O'Sullivan O, Wang Q, Nikkila J, Marchesi JR, Smidt H, de 775 Vos WM, Ross RP, O'Toole PW. 2009. Comparative analysis of pyrosequencing 776 and a phylogenetic microarray for exploring microbial community structures in 777 the human distal intestine. PLoS One 4:e6669. 778 35. Meyer F, Paarmann D, D'Souza M, Olson R, Glass EM, Kubal M, Paczian T, 779 Rodriguez A, Stevens R, Wilke A, Wilkening J, Edwards RA. 2008. The 780 metagenomics RAST server - a public resource for the automatic phylogenetic 781 and functional analysis of metagenomes. BMC Bioinformatics 9:386. 782 36. Coplen TB. 1996. Atomic weights of the elements 1995. Pure and Applied 783 Chemistry 68:2339–2359. 784 37. (CODATA) CoDfSaT. 2015. The NIST Reference on Constants, Units, and

Uncertainty, on National Institute of Standards and Technology. Accessed July 2,

787 38. R Development Core Team. 2014. R: A language and environment for 788 statistical computing, on R Foundation for Statistical Computing. http://www.R-789 project.org/. Accessed 15 Aug 2015 790 39. Rangel-Castro JI, Killham K, Ostle N, Nicol GW, Anderson IC, Scrimgeour 791 CM, Ineson P, Meharg A, Prosser JI. 2005. Stable isotope probing analysis of 792 the influence of liming on root exudate utilization by soil microorganisms. 793 Environmental Microbiology 7:828-838. 794 40. Kovatcheva-Datchary P, Egert M, Maathuis A, Rajilic-Stojanovic M, de 795 Graaf AA, Smidt H, de Vos WM, Venema K. 2009. Linking phylogenetic 796 identities of bacteria to starch fermentation in an in vitro model of the large 797 intestine by RNA-based stable isotope probing. Environmental Microbiology 798 **11:**914-926. 799 41. Darjany LE, Whitcraft CR, Dillon JG. 2014. Lignocellulose-responsive 800 bacteria in a southern California salt marsh identified by stable isotope probing. 801 Frontiers in Microbiology 5: 263 802 42. Hu HW, Macdonald CA, Trivedi P, Holmes B, Bodrossy L, He JZ, Singh BK. 803 2015. Water addition regulates the metabolic activity of ammonia oxidizers 804 responding to environmental perturbations in dry subhumid ecosystems. 805 Environmental Microbiology **17:**444-461. 806 43. Jiang XJ, Hou XY, Zhou X, Xin XP, Wright A, Ji ZJ. 2015. pH regulates key 807 players of nitrification in paddy soils. Soil Biology & Biochemistry 81:9-16. 808 44. Brenna JT, Corso TN, Tobias HJ, Caimi RJ. 1997. High-precision continuous-

flow isotope ratio mass spectrometry. Mass Spectrometry Reviews 16:227-258.

810 45. Amelung W, Brodowski S, Sandhage-Hofmann A, Bol R. 2008. Ccombining 811 biomarker with stable isotope analysis for assessing the transformation and 812 turnover of soil organic matter, p 155-250. In Sparks DL (ed), Advances in 813 Agronomy, Vol 100, vol 100. 814 46. Kramer C, Gleixner G. 2008. Soil organic matter in soil depth profiles: Distinct 815 carbon preferences of microbial groups during carbon transformation. Soil 816 Biology & Biochemistry 40:425-433. 817 47. Treonis AM, Ostle NJ, Stott AW, Primrose R, Grayston SJ, Ineson P. 2004. 818 Identification of groups of metabolically-active rhizosphere microorganisms by 819 stable isotope probing of PLFAs. Soil Biology & Biochemistry **36:**533-537. 820 48. Pett-Ridge J, Weber PK. 2012. NanoSIP: NanoSIMS applications for microbial 821 biology. Methods in molecular biology (Clifton, NJ) 881:375-408. 822 49. Mayali X, Weber PK, Brodie EL, Mabery S, Hoeprich PD, Pett-Ridge J. 823 2012. High-throughput isotopic analysis of RNA microarrays to quantify 824 microbial resource use. Isme Journal 6:1210-1221. 825 50. Orphan VJ, House CH, Hinrichs KU, McKeegan KD, DeLong EF. 2001. 826 Methane-consuming archaea revealed by directly coupled isotopic and 827 phylogenetic analysis. Science 293:484-487. 828 51. Behrens S, Losekann T, Pett-Ridge J, Weber PK, Ng WO, Stevenson BS, 829 Hutcheon ID, Relman DA, Spormann AM. 2008. Linking microbial phylogeny 830 to metabolic activity at the single-cell level by using enhanced element labeling-831 catalyzed reporter deposition fluorescence in situ hybridization (EL-FISH) and

NanoSIMS. Applied and Environmental Microbiology 74:3143-3150.

833 52. Urbach E, Vergin KL, Giovannoni SJ. 1999. Immunochemical detection and 834 isolation of DNA from metabolically active bacteria. Applied and Environmental 835 Microbiology 65:1207-1213. 836 53. Goldfarb KC, Karaoz U, Hanson CA, Santee CA, Bradford MA, Treseder 837 KK, Wallenstein MD, Brodie EL. 2011. Differential growth responses of soil 838 bacterial taxa to carbon substrates of varying chemical recalcitrance. Frontiers in 839 Microbiology 2. 840 54. Hellman M, Berg J, Brandt KK, Hallin S. 2011. Survey of bromodeoxyuridine 841 uptake among environmental bacteria and variation in uptake rates in a 842 taxonomically diverse set of bacterial isolates. Journal of Microbiological 843 Methods 86:376-378. 844 55. Nannipieri P, Ascher J, Ceccherini MT, Landi L, Pietramellara G, Renella 845 G. 2003. Microbial diversity and soil functions. European Journal of Soil Science 846 **54:**655-670. 847 56. Stotzky G, Norman AG. 1961. Factors limiting microbial activities in soil. 848 Archiv fur Mikrobiologie 40:341-369. 849 57. Manefield M, Griffiths RI, Bailey MJ, Whiteley AS. 2006. Stable isotope 850 probing: A critique of its we in linking phylogeny and function. Nucleic Acids 851 and Proteins in Soil 8:205-216. 852 58. Blazewicz SJ, Schwartz E. 2011. Dynamics of O-18 Incorporation from H (2) 853 (18) O into Soil Microbial DNA. Microbial Ecology 61:911-916. 854 59. Schwartz E. 2007. Characterization of growing microorganisms in soil by stable

isotope probing with H218O. Appl Environ Microbiol 73:2541-2546.

878

Ecology 83:402-412.

856 60. Nannipieri P, Johnson RL, Paul EA. 1978. Criteria for measurement of 857 microbial-growth and activity in soil. Soil Biology & Biochemistry 10:223-229. 858 61. McMahon SK, Wallenstein MD, Schimel JP. 2009. Microbial growth in Arctic 859 tundra soil at-2 degrees C. Environmental Microbiology Reports 1:162-166. 860 62. Bernard L, Mougel C, Maron PA, Nowak V, Leveque J, Henault C, Haichar 861 FZ, Berge O, Marol C, Balesdent J, Gibiat F, Lemanceau P, Ranjard L. 862 2007. Dynamics and identification of soil microbial populations actively 863 assimilating carbon from 13C-labelled wheat residue as estimated by DNA- and 864 RNA-SIP techniques. Environ Microbiol 9:752-764. 865 63. Haichar FZ, Achouak W, Christen R, Heulin T, Marol C, Marais MF, 866 Mougel C, Ranjard L, Balesdent J, Berge O. 2007. Identification of cellulolytic 867 bacteria in soil by stable isotope probing. Environ Microbiol 9:625-634. 868 64. Nottingham AT, Griffiths H, Chamberlain PM, Stott AW, Tanner EVJ. 869 2009. Soil priming by sugar and leaf-litter substrates: A link to microbial groups. 870 Applied Soil Ecology 42:183-190. 871 65. Peterson BJ, Fry B. 1987. Stable Isotopes in Ecosystem Studies. Annual Review 872 of Ecology and Systematics 18:293-320. 873 66. Schimel DS. 1993. Isotopic Techniques in Plant, Soil and Aquatic Biology: 874 Theory and application of tracers. 875 Mayali X, Weber PK, Pett-Ridge J. 2013. Taxon-specific C/N relative use 67. 876 efficiency for amino acids in an estuarine community. FEMS Microbiology

879 Figure Legends 880

Figure 1. Conceptual model of the quantitative stable isotope probing technique, from sample collection to determining the density of 16S rRNA gene fractions for individual taxa and their corresponding values of atom % stable isotope composition. Note: except for the addition of the stable isotope tracer at the beginning of the incubation, all steps are applied identically to both labeled and unlabeled samples. Artwork by Victor Leshyk.

885

886

887

888

889

890

881

882

883

884

Figure 2 (A) The ¹⁸O composition of E. coli DNA as a function of the ¹⁸O composition of water in the growth medium. Solid line is the regression ($^{18}O_{DNA} = 0.3339 \text{ x}$ $^{18}O_{H2O} +$ 0.0004, n=15, P<0.001, R²=0.976). (B) The average density of E. coli DNA as a function of the 18 O composition of the DNA (density = 0.0644 x atom fraction 18 O + 1.6946 $R^2 = 0.852, n=15$

891

892

893

894

895

896

897

898

899

900

901

Figure 3. The relative abundance of bacterial 16S rRNA genes, measured through quantitative PCR, as a function of density of DNA. Isotope treatments are shown with filled symbols while natural abundance controls are shown with open symbols. Comparison of soil samples incubated with (A) ¹²C-glucose and ¹³C-glucose, (B) ¹⁶O- $\rm H_2O$ and $\rm ^{18}O$ - $\rm H_2O$, and (C) $\rm ^{16}O$ - $\rm H_2O$ plus $\rm ^{12}C$ -glucose and $\rm ^{18}O$ - $\rm H_2O$ plus $\rm ^{12}C$ -glucose. The dotted lines represent the density that separates labeled from non-labeled DNA in traditional SIP. The distribution of densities in each replicate tube yielded an estimate of the average density for that tube, indicated by the horizontal position of the large symbols and error bars at the top of each panel (bars show 90% CIs, with n=3; the vertical position of these symbols does not convey meaning).

903

904

905

906

907

908

909

910

911

912

913

914

915

916

917

918

919

920

921

922

923

924

Bars show bootstrapped medians and 90% CIs.

Figure 4. Frequency distribution of the 16S rRNA gene as a function of density of DNA for three bacterial taxa without added glucose (left panels) and with added (natural abundance δ^{13} C) glucose (right side panels) for three different taxa: unidentified genera in the families Micrococacceae (A & B) and Pseudonocardiaceae (C & D), and genus Herpetosiphonales (E & F). Open symbols and dashed lines show the density distribution for the incubation where all substrates had natural abundance isotope composition, and filled symbols and solid lines show the distribution with ¹⁸O-water. Different shapes represent individual replicates within a treatment combination. For each replicate, the area under the curve sums to 1. The distribution of densities for each taxon in each replicate yielded an estimate of the average density for that taxon, indicated by the horizontal position of the large symbols and error bars at the top of each panel (bars show 90% CIs, with n=3; note, the vertical position of the large symbols does not convey meaning). Figure 5. The taxon-specific shift in average density of DNA (g cm⁻³, lower horizontal axis) and the corresponding atom fraction excess of ¹⁸O or ¹³C (upper horizontal axis) between incubations with enriched and natural abundance substrates. Changes in DNA density were caused by ¹⁸O incorporation from water (A) without or (B) with added natural abundance glucose, or by (C) ¹³C incorporation from added ¹³C-labeled glucose.

Figure 6. Atom fraction ¹³C with added ¹³C-glucose and the shift in atom fraction ¹⁸O caused by added ¹²C-glucose across groups of bacteria. The solid black line represents the expected relationship if organisms derived 100% of their carbon from the added glucose and 33% of their oxygen from ¹⁸O water. The difference between the solid line and points falling above it is the indirect effect of added glucose on the utilization of other carbon substrates, reflecting the difference between the total growth stimulation caused by glucose addition and the stimulation based on direct reliance on the added glucose. Points show means with standard errors of the mean (n=3).

933

925

926

927

928

929

930

931

934	rable 1. Dell	initions of indices, variables, and calculated quantities used in inodeling excess atom fraction. O for each bacterial taxof
935	Indices:	
936	i	taxon
937	j	replicate (or tube) within a treatment
938	k	fraction (within a replicate)
939	I	number of taxa
940	J	number of replicates (within a treatment)
941	K	number of fractions (within a replicate)
942		
943	Variables:	
944	f_{jk}	total number of 16S rRNA gene copies per μ L (all taxa combined) in fraction k of replicate j (copies μ L ⁻¹)
945	p_{ijk}	proportion of the total number of 16S rRNA gene copies per μ L that are taxon i in fraction k of replicate j (unitless)
946	x_{jk}	density of fraction k of replicate j (g cm ⁻³)
947		
948	Calculated qu	uantities:
949	y_{ijk}	number of 16S rRNA gene copies per μ L of taxon i in fraction k of replicate j (copies μ L ⁻¹)

950	Уij	total number of 16S rRNA gene copies per μ L of taxon i in replicate j (copies μ L ⁻¹)	
951	W_{ij}	observed weighted average density for taxon i in replicate j (g cm ⁻³)	
952	W_{LABi}	mean observed weighted average density for $taxon i$ in the labeled treatment (mean across all replicates of the treatment	
953		with the heavy isotope) (g cm ⁻³)	
954	W_{LIGHTi}	mean observed weighted average density for $taxon i$ in the unlabeled (i.e., natural abundance) treatment (mean across	
955		all replicates in all treatments without heavy isotopes) (g cm ⁻³)	
956	G_i	guanine + cytosine content of taxon i (unitless)	
957	$H_{CARBONi}$	average number of carbon atoms per DNA nucleotide for taxon i	
958	M_{LIGHTi}	observed molecular weight of the DNA fragment containing the 16S RNA gene for taxon i in the unlabeled (i.e.,	
959		natural abundance) treatment (g mol ⁻¹)	
960	$M_{HEAVYMAXi}$	theoretical molecular weight of the DNA fragment containing the 16S RNA gene for taxon i assuming maximum	
961		labeling by the heavy isotope (g mol ⁻¹)	
962	M_{LABi}	observed molecular weight of the DNA fragment containing the 16S RNA gene for taxon i in the labeled treatment (g	
963		mol ⁻¹)	
964	Z_i	difference in observed weighted average densities of taxon i for the labeled and unlabeled treatments (g cm ⁻³)	
965	$A_{OXYGENi}$	excess atom fraction of 18 O in the labeled versus unlabeled treatment for taxon i (unitless)	

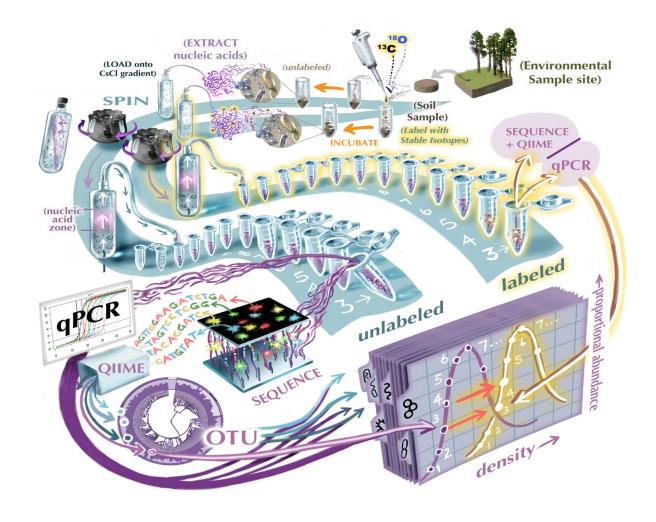
Applied and Environmental Microbiology

excess atom fraction of 13 C in the labeled versus unlabeled treatment for taxon i (unitless) 966 $A_{CARBONi}$

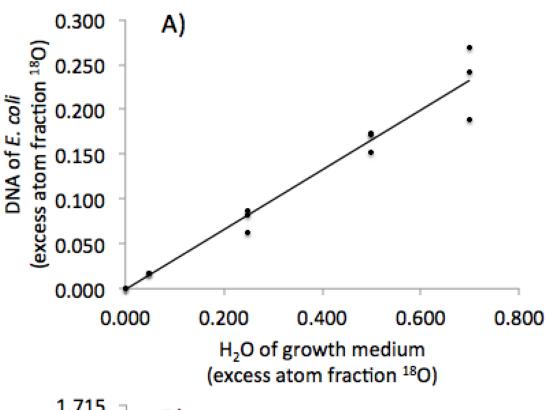
48

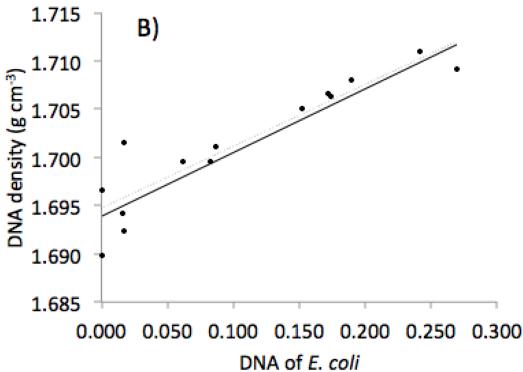
Table 2. Density (g cm⁻³) of DNA for taxa exhibiting or not exhibiting tracer assimilation in the three tracer experiments. Values are means and standard deviations.

	Density (g cm ⁻³)		
Tracer	assimilating	not assimilating	
¹⁸ O-H ₂ O	1.6905 ± 0.0031	1.6912 ± 0.0033	
¹⁸ O-H ₂ O with glucose	1.6896 ± 0.0033	1.6894 ± 0.0045	
¹³ C-glucose	1.6890 ± 0.0030	1.6900 ± 0.0036	









(excess atom fraction 18O)

